The transcription factor SOX6 contributes to the developmental origins of obesity by promoting adipogenesis

Shi Chi Leow[1], Jeremie Poschmann[2], Peh Gek Too[1], Juan Yin[3], Roy Joseph[1], Craig McFarlane[1], Shaillay Dogra[1], Asim Shabbir[4], Philip W. Ingham[3,5], Shyam Prabhakar[2], Melvin K.S. Leow[1,6], Yung Seng Lee[1,7], Kai Lyn Ng[8], Yap Seng Chong[1,8], Peter D. Gluckman[1,9] & Walter Stünkel[1]

[1]Singapore Institute for Clinical Sciences, Agency for Science Technology and Research (A*STAR)
[2]Genome Institute of Singapore, Agency for Science Technology and Research (A*STAR)
[3]Lee Kong Chian School of Medicine, Nanyang Technological University, Singapore
[4]Department of Surgery, National University Hospital, National University of Singapore
[5]Institute of Molecular and Cell Biology, Agency for Science Technology and Research (A*STAR)
[6]Department of Endocrinology, Tan Tock Seng Hospital, Singapore
[7]Department of Paediatrics, Yong Loo Lin School of Medicine, National University of Singapore
[8]Department of Obstetrics and Gynaecology, Yong Loo Lin School of Medicine, National University of Singapore
[9]Liggins Institute, University of Auckland, New Zealand

Corresponding author:
Dr. Walter Stünkel
Brenner Centre for Molecular Medicine
30 Medical Drive
Singapore 117609
Phone: +65-64070689/Fax: +65-67766840
e-mail: Walter_Stunkel@sics.a-star.edu.sg

Abstract

The association between impaired fetal growth and postnatal development of obesity has been demonstrated before. By comparing adipocytes differentiated from Mesenchymal Stem Cells (MSCs) taken from the umbilical cord and derived from normal and growth restricted neonates, we identified the transcription factor SOX6 as a highly expressed gene only in growth restricted individuals. We found that SOX6 regulates the process of adipogenesis in vertebrate species by activating adipogenic regulators including PPARγ, C/EBPα, and MEST. We further show that SOX6 interacts with β-catenin in adipocytes suggesting an inhibition of WNT/β-catenin signaling thereby promoting adipogenesis. The upstream regulatory region of the MEST gene in MSCs from growth restricted subjects harbors hypo-methylated CpGs next to SOX6 binding motifs and we found that SOX6 binding is impaired by adjacent CpG methylation. In summary, we report that SOX6 is a novel regulator of adipogenesis synergizing with epigenetic mechanisms.

Introduction

Obesity is becoming increasingly prevalent and contributes to morbidity and mortality worldwide (Ng et al., 2014; Bhurosy et al., 2014). Although there is little doubt that it can result from adult lifestyle factors, there is increasing evidence for developmental factors playing an important role and these appear to operate through epigenetic pathways (van Dijk et al., 2015). Indeed there is compelling evidence supporting the concept that the origins of obesity often begin in utero (Desai et al., 2005; de Rooij et al., 2007) and impaired fetal growth has been linked to the development of obesity and metabolic diseases in adult life (Godfrey and Barker, 2001; Kensara et al., 2006). The role of low birth weight in the development of human adult non-communicable diseases has been described before (Lackland et al., 2000; Tian et al., 2006). In particular, infants with low birth weight and fetal growth restriction combined with accelerated catch-up in the first few years of life are at higher risk of developing obesity (Khandelwal et al., 2014; Varvarigou, 2010).

The mechanistic pathway by which impaired intrauterine conditions induce later sensitivity to an obesogenic environment has been extensively reviewed elsewhere (Hanson and Gluckman, 2014) and there is clinical evidence suggesting epigenetic mechanisms are involved (Godfrey et al., 2011). To explore molecular mechanisms that may be important in this relationship, we previously reported the use of multipotent Mesenchymal Stem Cells (MSCs) from the Wharton's jelly of umbilical cord (UC) tissue to generate primary UC-MSC isolates from small for gestational age (SGA) and normal neonates (Sukarieh et al., 2014). Chromatin Immunoprecipitation-Sequencing (ChIP-seq) studies from adipocytes differentiated from MSCs revealed candidate genes that were found to be associated with histone hyper-acetylation and increased gene expression in the SGA group (Joseph et al., 2015). One gene of uncertain functional importance found in that study was SOX6 (SRY (Sex Determining Region Y)-Box 6). Here, we describe effects of SOX6 on adipogenesis and demonstrate putative molecular mechanisms by showing that SOX6 regulates the expression of key adipogenic regulators, and synergizes with epigenetic pathways involving MEST (Mesoderm Specific Transcript), a known associate of adipocyte size (Takahashi et al., 2005) and adipose tissue expansion with as yet unknown biochemical functions (Voigt et al., 2015). Epigenetic changes within the MEST promoter have been

previously associated with maternal stress leading to adverse birth outcomes (Vidal et al., 2014). Our results show that epigenetic properties of the MEST gene upstream regulatory region synergize with SOX6 function in positively regulating adipogenesis in MSCs isolated from SGA individuals.

Results

SOX6 is highly expressed in MSC derived-adipocytes from SGA neonates

In our previous study, histone ChIP-seq using preadipocytes (cycle 0), intermediate (cycle 3) and mature differentiated adipocytes (cycle 6) from two representative cell lines of SGA (MSC-01) and control group neonates (MSC-44) revealed notably different enrichment of H3K27 acetylation sites in adipocytes derived from SGA background (Joseph et al., 2015). SOX6 was found to be one of the most significant genes with promoter associated histone H3K27 acetylation along with lower levels of H3K27 trimethylation in adipocytes derived from the MSC-01 SGA compared to the MSC-44 control isolate (Fig. 1A). We evaluated the expression pattern of SOX6 in adipocytes derived from both MSC-01 and MSC-44 (Fig. 1B) as well as adipocytes derived from an extended larger group of primary SGA and control MSC isolates (Fig. 1C, supplementary material Table S2). We found that SOX6 gene expression levels were significantly higher in adipocytes with SGA background. Correspondingly, similar observations were made for known adipogenic genes such as PPARγ, C/EBPα, FABP4 and FASN (supplementary material Fig. S1C), in line with our published observations of a higher adipogenic potential for differentiated MSCs derived from the SGA group (Joseph et al., 2015). Western blots showing the protein levels of SOX6 in the adipocytes (Fig. 1D) confirmed our qRT-PCR findings and correlated well with the transcriptional state predicted by the ChIP-seq data set.

Modulation of SOX6 expression regulates adipocyte differentiation and triglyceride levels

A function for SOX6 in human adipocyte differentiation has not been previously reported and in order to test the hypothesis that SOX6 exerts an effect on adipocyte differentiation, we performed siRNA-

mediated SOX6 knockdown experiments with several differentiated primary human Wharton's jelly derived MSC-, as well as adipose stromal cell (ASC) lines. Silencing SOX6 expression reduced the formation of lipid droplets in both human cell lines (MSC-01, Fig. 2A and APOD-01, Fig. 2B). These results were concordant with triglyceride levels measured in the same samples (Figs. 2C and 2D). Similar results were obtained in mouse 3T3L1 adipocytes (supplementary material Fig. S1A), as well as in additional human ASC and MSC lines (supplementary material Figs. S1B and S2A, supplementary material Table S2). We also applied the reverse approach by transfecting a SOX6 expression vector into 3T3L1 preadipocytes and observed a significant increase in cellular triglyceride levels compared to the GFP control vector at day 4 of adipogenesis (supplementary material Fig. S1D).

To confirm that the inhibition of adipogenesis was specifically due to SOX6 inhibition, we measured the mRNA expression of other SOX family members such as SOX5, SOX9 and SOX13 following the siRNA mediated SOX6 depletion. As shown in Supplementary Figures 2B and 2C, inhibition of SOX6 did not lead to significant changes in the expression of other members of the SOX family.

SOX6 enhances adipogenesis by directly regulating the expression of adipogenic genes

In order to gain mechanistic insights into the effects of SOX6 on adipogenesis, we examined the expression patterns of key adipocyte markers in fully differentiated adipocytes. Knockdown of SOX6 led to a reduction in the expression of MEST, FABP4, FASN, GLUT4, PPARγ and C/EBPα in MSC-01 cells (Figs 3A-C), in all ASC derived adipocytes (supplementary material Figs. S3A and S3B) and in 3T3L1 cells (supplementary material Figs. S4A and S4B). PPARγ and C/EBPα are critical transcription factors required for adipogenesis (Rosen et al., 2002), and the expression of these factors is dependent on the expression of adipogenic initiation factors including C/EBPβ and C/EBPδ. Quantitative PCR analyses showed that C/EBPβ was down-regulated by SOX6 depletion in MSC-01 at cycle 0 (Fig. 3B), in ASC lines (supplementary material Figs. S3A and S3B, right panels), and in 3T3L1 pre-adipocytes (supplementary material Fig. S4A, right panel). C/EBPδ expression was not affected in 3T3L1 and MSC-01 cells, but significantly downregulated in the adult human ASC lines

(supplementary material Figs. S3A and S3B, right panels). These findings indicate that SOX6 mediates adipocyte differentiation and lipogenesis by upregulating the adipogenic signaling cascade, specifically increasing adipocyte expression of PPARγ and CEBPα, FABP4, as well as MEST. In light of our earlier findings, we further examined whether SOX6 can directly regulate the expression of MEST and PPARγ by performing ChIP using preadipocytes (cycle 0 / day 0), intermediate (cycle 3 / day 4) and mature differentiated adipocytes (cycle 6 / day 8) derived from MSC-01 and 3T3L1 cells. Allowing one base deviation from the SOX6 binding motif (WWCAAWG), we identified 17 potential SOX6 binding sites 1kb upstream of the MEST gene and designed 3 sets of primers to test selected sites (Fig. 3D) in MSC-01 cells. We confirmed that under differentiating conditions, SOX6 was found to be enriched at the MEST promoter region (Fig. 3E). Similarly, we observed stronger enrichment of SOX6 at the MEST promoter region in differentiating 3T3L1 cells compared to fully differentiated cells at day 8 (supplementary material Fig. S4C). Our ChIP analysis also demonstrated that endogenous SOX6 binds to the PPARγ promoter region (Fig. 3E supplementary material Fig S4C), indicating that also PPARγ is a direct downstream target of SOX6. In order to further support the hypothesis that SOX6 directly regulates expression of the MEST and PPARγ genes by direct promoter binding, we conducted gene specific luciferase reporter assays during the differentiation of 3T3L1 cells. In both cases, the siRNA mediated Sox6 knockdown reduced reporter gene activity (supplementary material Figs. S4D and S4E, respectively).

CpGs within the MEST promoter are hypo-methylated in differentiated adipocytes from SGA neonates and facilitate the binding of SOX6

Having established a role of SOX6 as an activator of adipogenesis, we aimed to get more mechanistic insights into the mechanisms of SOX6 action in the context of developmental induction of a greater propensity to obesity. We specifically addressed the question whether potential synergisms between SOX6 over-expression and other molecular pathways can be found in Wharton's jelly derived MSCs. There are numerous examples demonstrating an impairment of transcription factor binding by site specific CpG-methylation (Cho et al., 2013). In order to investigate whether similar mechanisms exist for some of the downstream targets of SOX6, we assessed the methylation status of CpG

dinucleotides adjacent to putative SOX6 binding sites within the MEST upstream gene regulatory region. As depicted in Fig. 4A, we selected 6 candidate sites (CpGs A-F) near the MEST transcriptional start site surrounding 3 putative SOX6 binding sites (open boxes) and determined their methylation status via pyrosequencing. We compared 5 adipocyte cell lines differentiated from Wharton's jelly MSCs taken from the control group and 7 corresponding lines from the SGA group. All CpG sites showed a significant decrease in methylation levels in the SGA group compared to the controls (Fig. 4B). Hypo-methylation of this region in the SGA group of adipocyte cell lines was accompanied by an increased expression of MEST (Fig. 4C) indicating a functional relationship between CpG methylation and gene expression levels in the two groups. To examine the mechanistic basis for the above relationship, we conducted electrophoretic mobility shift assays (EMSA) comparing methylated and non-methylated MEST probes covering the CpG B site next to a SOX6 binding motif. We found that CpG methylation at this site interferes with SOX6 binding (Fig. 4D), which may explain the lower expression of MEST in adipocytes from normal control MSCs and enhanced SOX6 binding in adipocytes from SGA neonates.

SOX6 inhibits WNT/β-catenin signaling in adipocytes

We observed that SOX6 promotes MEST expression and that SOX6 expression was found to increase during adipocyte differentiation. We therefore investigated the possibility of SOX6 regulating the WNT signaling pathway and showed that ectopic expression of SOX6 attenuates WNT3a-CM (conditioned medium)-mediated reporter activity (Fig. 5A). To demonstrate the interaction between β-catenin and SOX6, we conducted a co-immunoprecipitation experiment showing that SOX6 interacts with β-catenin (Figs. 5B and C). Furthermore, decreasing SOX6 expression in 3T3L1 during differentiation increased the protein levels of β-catenin (Fig. 5D). Similarly, treatment of cells with the specific proteasome inhibitor MG132 abolished the SOX6-mediated reduction in total cellular β-catenin levels, and its transcriptional target gene Axin2 (Fig. 5E). These findings indicate that SOX6 depletion may alleviate suppression of the canonical β-catenin branch of the WNT signaling pathway by promoting proteasomal degradation of β-catenin.

SOX6 regulates lipid metabolism in vivo

In order to further establish the role of SOX6 in mediating adipogenesis *in vivo*, we investigated the effect of reducing SOX6 levels in C57BL/6 mice using Locked Nucleic Acid antisense oligonucleotides (LNA ASOs). Sox6-specific ASO treatment was effective in decreasing Sox6 mRNA expression in epididymal white adipose tissues and significantly decreased the expression of Pparg, C/ebpa and adiponectin (Fig. 6A). We also confirmed the Sox6 knockdown in liver and epididymal white adipose tissue, EWAT, (Fig. 6B and supplementary Fig. S5 A and B). We then measured the lipid profiles and observed that Sox6 ASO treatment reduced serum- and liver triglyceride (Figs. 6C and D), as well as serum cholesterol levels (Fig. 6E). Serum levels of several adipokines including leptin and adiponectin correlate with adiposity and imbalances in their secretion may promote obesity-associated metabolic changes (Maury and Brichard 2010). Serum leptin levels were significantly reduced in Sox6 ASO-treated mice (Fig. 6F), consistent with the known positive correlation of leptin levels with fat mass (Considine et al., 1996). Serum levels of adiponectin, however, were not found to be significantly different in the Sox6 ASO-treated mice compared to the controls (Fig. 6G), suggesting that adiponectin secretion in the blood serum did not contribute to the metabolic phenotype of the Sox6-deficient mice. To identify additional downstream target genes of Sox6 in the liver, we conducted a gene expression microarray study comparing livers from the control and Sox6 ASO-treated mice for future validation of liver specific functions of Sox6. From the microarray data set we selected the most significantly expressed genes and validated their expression levels by qRT-PCR. We confirmed up-regulation of genes Mknk2 and Upp2 ($p \leq 0.001$), as well as significant down-regulation of genes encoding Pmvk, Fabp5, Immp2l, Nfat5, Dapk1, Ube2e1, Acss2, Acacb and Fasn ($p \leq 0.001$, supplementary material Fig. S5 C).

Loss of Sox6 decreases adipogenesis in zebrafish larvae

To address potential conservation of Sox6 function in adipocyte differentiation across vertebrate species, we used the zebrafish as an experimental model. The optical transparency of the zebrafish larva facilitates the visualization of adipocytes by Nile Red staining in whole mount preparation

(Flynn et al., 2009). Loss of Sox6 function in zebrafish has previously been shown to disrupt the differentiation of fast-twitch skeletal muscle fibers, but effects on adipocytes have previously not been addressed (Jackson et al., 2015). For the current study, control and sox6 homozygous null mutant larvae were stained with Oil Red O (Fig. 7A) or Nile Red (Fig. 7B) to reveal the localization of adipocyte neutral lipid droplets. Lipid droplets were reduced both in number and size in the Sox6 mutants (Fig. 7A, middle panel, quantification of the lipid contents shown on the right, and Fig. 7B, right panel). The number of neutral lipid droplets was found to be decreased in Sox6 null mutants at all developmental stages (Fig. 7C).

Discussion

The process of adipogenesis has been well studied and most master regulators have been identified. These include PPARγ and various members of the C/EBP family of transcription factors (Lefterova et al., 2014). We have described for the first time that the transcription factor SOX6 acts as an activator of adipogenesis upstream of PPARγ and MEST by direct binding to and activation of their promoters. SOX6 is a group D member of the SOX family of proteins including SOX5 and SOX13 (Lefebvre et al., 2001), and the essential roles of the multifaceted transcription factor SOX6 in cell differentiation have been demonstrated in studies comprising myocytes (Hagiwara et al., 2007), oligodendrocytes (Stolt et al., 2006), chondrocytes (Smits et al., 2001), neurons (Batista-Brito et al., 2009), and erythroblasts (Dumitriu et al., 2006). Whilst it's possible role in regulating insulin secretion in pancreatic β-cells is reported (Iguchi et al., 2005), our data suggest a direct metabolic function for SOX6 in regulating the triglyceride content in white adipose- and liver tissues. This effect is evolutionary conserved amongst vertebrates, as our data from Sox6 -/- mutant zebrafish show. The mechanism of action may differ in a tissue specific manner, but in adipocytes, in addition to the direct regulation of PPARγ and C/EBP expression, we showed that SOX6 inhibits WNT signaling by binding to β-catenin potentially leading to its degradation (Fig. 8). Our data from differentiated adipocytes reveal that this interaction involves proteasomal degradation of β-catenin with subsequent inhibition of β-catenin/TCF signaling. As the WNT pathway is known to inhibit adipogenesis (Ross et al., 2000; Kennell et al., 2005), SOX6 therefore counteracts this negative influence and promotes adipocyte differentiation. But the interaction with β-catenin is not the only way in which SOX6 can act upon WNT signaling. One of the key molecular associates of adipocyte size is the gene MEST and we identified a strong effect of SOX6 depletion on MEST expression levels, which can be further explained by our data revealing a direct binding of SOX6 to binding sites within the MEST promoter. MEST has been reported to inhibit the WNT/β-catenin signaling pathway by sequestering β-catenin (Li et al., 2014) and through glycosylation of LRP6 (Jung et al., 2011). MEST is also known as PEG1 (paternally expressed gene 1), an imprinted gene with expression from the paternal allele (Kamei et al., 2007) and probable developmental functions of MEST could complement those of SOX6. At

present, we do not understand which factors promote SOX6 up-regulation in SGA derived adipocytes, apart from the strong association with hyper-acetylated histones. But higher SOX6 expression levels in adipocytes from SGA individuals may synergize with MEST hypo-methylation at CpGs found next to putative SOX6 binding sites. Decreased CpG methylation within the MEST promoter may facilitate SOX6 binding thereby enhancing MEST expression, which in turn will stimulate lipogenesis and adipocyte growth. This model is supported by our EMSA data demonstrating impaired SOX6 binding to a MEST promoter template with adjacent CpG methylation. Our findings therefore extend published observations that obesity significantly associates with decreased methylation levels at the MEST gene (Soubry et al., 2015), that MEST hypo-methylation is linked to metabolic programming in offspring with background in gestational diabetes (El Hajj et al., 2013), and that there is an inverse relation between MEST CpG methylation levels and body composition measures such as waist circumference and body mass index (Carless et al., 2013).

We previously published the observations of significant molecular changes in Wharton's jelly derived MSCs from SGA infants prior (Sukarieh et al., 2014), and post adipocyte differentiation (Joseph et al., 2015). Given its evolutionary importance and demonstration in multiple species (Hanson and Gluckman, 2014), it seems probable that multiple molecular pathways operate to predispose individuals with a history of suboptimal early-life conditions to later increased metabolic disease risk. However, our study cannot prove beyond any reasonable doubt a direct role for SOX6 in directing the fetal origins of human obesity, but in concert with other likely mechanisms such as its direct effects on PPARγ expression and WNT signaling, SOX6 may be considered to be a key candidate in such processes.

The basic functions of SOX6 in adipogenesis are conserved between humans and other vertebrates, as shown by our cell line-(3T3L1), as well as in vivo data (mouse and zebrafish). Future research will address in more detail the mechanisms underlying the deregulation of SOX6 expression levels in the context of fetal growth restriction.

Materials and Methods

Clinical populations and sample collection

Fresh umbilical cords were obtained from children born at the National University Hospital (NUH), Singapore. IRB approval by the National University Health System (NUHS) was granted before cord collection. Prior written parental consent to participate in this study was obtained and ethical approval obtained by the Domain Specific Review Board (DSRB, # 2011/00355) of NUH.

Collection and establishment of human Adipose Stromal Cell (ASC) lines

Prior written consent to participate in this study was obtained and ethical approval was granted by the Domain Specific Review Board (DSRB, #2013/00171) of NUH. Human subcutaneous white adipose tissues (WAT) were obtained from two morbidly obese patients who underwent either laparoscopic sleeve gastrectomy or Roux en Y gastric bypass (supplementary material Table S1). The ASC lines APOD-01 and APOD-02 were established according to standard procedures. Briefly, less than 1g of WAT was digested with 1mg/mL collagenase Type IA (Sigma C9891-1G) in 20mg/mL BSA for 90min at 37°C with shaking (120rpm). Cell pellets were collected by centrifugation at 800xg for 10min, and then re-suspended in 9ml of Red Blood Cell (RBC) lysis buffer for 10min. Cells were filtered through a 100µm cell strainer and re-suspended in growth medium, DMEM/F-12 GlutaMAX (Dulbecco's modified Eagle's medium, DMEM) containing 20% fetal bovine serum (FBS), 1% penicillin- streptomycin (P/S).

Assessment of fetal growth characteristics

Methods for the assessment of fetal growth characteristics in this study are published (Sukarieh et al., 2014; Joseph et al., 2015). In short, the SGA condition was diagnosed by ultrasonography and determined as growth between the 5^{th} and 10^{th} percentile when compared to a control reference population. Standard scans were conducted by trained ultrasonographers, using ultrasound machines (Aloka SSD- 4000, GE Voluson E8).

Preparation and propagation of Mesenchymal Stem Cells (MSCs) from human umbilical cord

The preparation and full characterization of the primary Mesenchymal Stem Cell (MSC) isolates used in this study has been reported (Fong et al., 2010; Sukarieh et al., 2014, Joseph et al., 2015). A brief overview of the characteristics of all primary cell isolates used here is provided in supplementary material Table S2. For all experiments described the primary cell lines were passaged up to 10 times.

Adipocyte differentiation

Wharton's jelly MSCs: The differentiation of MSCs is described (Joseph et al., 2015).

Human adipose stromal cells: Cells were plated into 3 cm or 6 cm dishes coated with 0.2% gelatin and grown in growth medium (DMEM/F-12 GlutaMAX, 20% FBS, antibiotic/antimycotic mixture). 2 days after reaching confluence (labelled as Day 0), the cells were stimulated to differentiate by culturing them in IBMX Induction Medium (DMEM/F-12 GlutaMAX (Invitrogen), 10% FBS (Hyclone), supplemented with 0.5 mM isobutylmethylxanthine (IBMX, Sigma I-7018), 1 µM dexamethasone (Sigma D-4902), 200 µM indomethacine (Sigma, I-8280) and 58 ug/ml insulin (bovine, Sigma I-5500), for 1 week with a replacement of fresh media every 2 days. After 1 week, the IBMX Induction Medium was replaced with Insulin Medium (DMEM/F-12 GlutaMAX (Invitrogen), 10% FBS (Hyclone), supplemented with 0.01mg/ml insulin). The insulin Medium was changed every 2 days. The siRNA knockdown was performed before differentiation and every 4 days during differentiation.

Mouse 3T3L1 cells: Cells were obtained from ATCC and plated into 3 cm or 6 cm dishes coated with 0.2% gelatin and grown in growth medium (DMEM high glucose with 2 mM L-glutamine, 10% FBS, antibiotic/antimycotic mixture) and allowed to grow to confluence for 2-3 days. The cells were then treated with Induction Medium (DMEM high glucose with 2 mmol/l L-glutamine, 10% FBS (Hyclone), supplemented with 0.5 mM isobutylmethylxanthine (IBMX, Sigma I-7018), 1 µM dexamethasone (Sigma D-4902), 0.01mg/ml insulin (Bovine, Sigma I-5500)), (Day 0) for 48hours. After 48 hours, the Induction Medium was replaced with insulin Medium (DMEM high glucose with

2 mmol/l L-glutamine, 10% FBS (Hyclone), supplemented with 0.01mg/ml insulin). The insulin Medium was changed every 2 days.

Oil Red O staining

Adipogenesis was quantified by Oil Red O staining following standard procedures. Briefly, the adipogenic cultures in 3 cm dishes were washed with PBS and fixed with 10% formaldehyde for 30-60 min at room temperature. The Oil Red O solution was prepared as a stock by dissolving 0.3 g powder in 100 ml isopropanol. 3 parts of Oil Red O stock solution were mixed with 2 parts DI water and allowed to sit at room temperature for 10 min before filtering. After adding the Oil Red O solution to the dishes, they were incubated for 10 min at room temperature. For whole mount zebrafish staining at larval stages, the larvae were fixed with 4% paraformaldehyde, rinsed with PBT (PBS/0.5% tween-20), and stained with filtered Oil red O solution for 15 min at room temperature. Stained larvae were rinsed three times with PBT, and twice with 60% isopropanol for 5 min each. Then, the larvae were briefly rinsed with PBT and re-fixed with 4% paraformaldehyde for 10 min. Finally, the larvae were mounted in 3% methylcellulose, and imaged using an AxioCam HRc mounted on a Zeiss AXIO Imager M2.

Nile Red staining

Nile Red (144-0811; Wako) was solubilized in acetone at a concentration of 1.25 mg/ml. It was subsequently kept at -20°C in the dark. Live zebrafish were placed in the egg water containing 0.5 ug/ml of Nile Red for 30 min in the dark. Zebrafish were then anesthetized using Tricaine (MS-222; Sigma-Aldrich), and mounted in 3% methylcellulose, followed by imaging using an AxioCam HRc mounted on a Zeiss AXIO Imager M2.

Chromatin Immunoprecipitation-sequencing (ChIP-seq) of histone H3K27-acetylation and –me3 marks and subsequent bioinformatics analysis

All procedures for the ChIP-seq study including all analytical steps are published (Joseph et al., 2015).

Chromatin Immunoprecipitation

In order to preserve protein-DNA complexes, 1% formaldehyde was added to the cells for 10 minutes at room temperature. The cross-link reactions were stopped by adding 125 mM glycine for 5 minutes and cells were incubated in SDS lysis buffer and subjected to sonication for 12 minutes with a Diagenode Bioruptor. Chromatin fragments were subsequently pre-cleared with protein A Sepharose beads (Invitrogen, 10-1142) and bovine serum albumin at 4°C for 2 hours prior to immunoprecipitation with SOX6, or rabbit control IgG antibodies overnight at 4°C. After washing and eluting the sepharose beads with SDS elution buffer, the cross-links were reversed by incubating the samples at 65°C overnight. Afterwards, the QIAquick PCR Purification Kit (Qiagen) was used for sample purification following the instructions of the manufacturer.

Quantitative ChIP-PCR analysis

For the data shown in Fig.3E, MEST and PPARγ promoter specific primers were used to analyze ChIP-enrichment using the ABI 7900 system (Perkin Elmer). The primer sequences are listed in supplementary Table S3.

Co-immunoprecipitation assay

Cells were washed with ice-cold PBS and subsequently lysed in 50 mM Tris, pH 8, 150 mM NaCl, 0.5% NP40, 0.5% deoxycholic acid, 0.005% SDS, as well as protease inhibitors for 30 minutes on ice. Samples were centrifuged and the supernatants incubated with either anti-SOX6 or anti-β-catenin or rabbit or mouse anti-IgG overnight at 4°C and with protein G sepharose beads (Invitrogen, 10-1243) for 2 hours. 500 µl PBS containing 0.1% Tween 20 were used to wash the beads up to four times. SDS sample buffer was used to elute all bound proteins, which were then separated by SDS-PAGE followed by immunoblotting with the specific antibodies stated.

RNA extraction

Cells were spun down in 1.7 ml tubes and re-suspended in 0.5 ml of TRIzol® Reagent (Life Technologies, 15596-026). All samples were snap-frozen on dry ice and stored at -80° C. RNA was

isolated and purified using the RNeasy Mini Kit (Qiagen, 74106) comprising the manufacturer's protocol.

Quantitative Real Time-PCR

For qRT-PCR, total RNA (1-2 µg) was reverse transcribed using a High Capacity cDNA Reverse Transcription Kit (Applied Biosystems Inc.). All cDNA samples were subjected to real-time PCR analysis (in triplicates) with gene specific primers (supplementary Table S3) using an ABI 7900 HT Sequence Detection System (Applied Biosystem Inc). Target gene expression levels were normalized to endogenous control genes (GAPDH or Ppia) and presented relative to the controls.

Animal studies

Rodents: All animals used were C57BL/6NTac mice purchased from BRC, A*STAR. All experimental procedures were approved by the Institutional Animal Care and Use Committee (IACUC). All mice were monitored daily for signs of morbidity. Whole blood was collected from cardiac puncture. For tissue collection, the mice were sacrificed according to IACUC guidelines, and the epididymal white adipose tissues and livers were collected for subsequent analysis.

Zebrafish: A 14 hour light/10 hour dark cycle at 28°C in the AVA (Singapore) certificated IMCB Zebrafish Facility was applied for the maintenance of adult fish. The zebrafish strain used in this study is Sox6i292, as described (Jackson et al., 2015).

ASO in vivo administration

Lyophilized LNA ASOs were produced according to the custom design generated by Exiqon's proprietary design software and were dissolved in sterile water. The sequences of the ASOs are available upon request. The re-suspended ASOs were then diluted in saline to the desired concentration required for dosing mice and sterilized through a 0.2 µm filter. Mice were anaesthetized with Avertin before ASOs were delivered via i.p. injection at a dose of 50 mg · kg−1 · week−1. After one week, the mice were sacrificed for blood and tissues collection.

Quantification of triglyceride content

Total soluble lipids from adipocytes differentiated from MSCs and 3T3L1 were extracted using the buffer provided with the commercial Adipogenesis Detection Kit (Abcam, ab102513) and samples were kept at -80°C until further analysis. Quantification of triglycerides was measured using the commercial Triglyceride Quantification kit (Abcam, ab65336) and carried out as per the manufacturer's instructions.

Quantification of cholesterol

Whole blood was obtained from mice using cardiac puncture. Blood was stored in a Sarstedt S-Monovette\® tubes containing serum gel. Serum was obtained by centrifuging the tubes at 10,000g, room temperature for 10 minutes. Liver samples from mice were snap-frozen and kept at -80°C until further analysis. The amount of total cholesterol was measured using the Cholesterol/Cholesteryl Ester Quantification Kit (Abcam, ab65359) using a colorimetric method as per the manufacturer's instructions.

Quantification of leptin and adiponectin

Serum levels of leptin and adiponectin were determined using ELISA, as per the manufacturer's instructions (R&D Systems, MOB00, MRP300).

Western Blotting

Differentiated adipocytes were harvested in RIPA buffer (50 mM TrisHCl pH7.4, 150 mM NaCl, 2 mM EDTA, 1% NP-40, 0.1% SDS). Membranes were probed with primary antibodies specific to SOX6 (Abcam,ab125196), MEST (Abcam, ab151564), β-catenin (BD Transduction Lab, 610153), Axin2 (Abcam, ab109307), PPARγ (Santa Cruz, sc7196), C/EBPα (Santa Cruz, c61), and FABP4 (Abcam, ab66682), and the endogenous control protein β-actin (Sigma, A1978). To inhibit proteasome mediated protein degradation, 2μM of MG132 (Sigma, C2211) was added to the cells.

The LICOR Odyssey 2.1 system was used for signal detection (secondary antibodies 926-32211, 926-68020) and band analysis.

SOX6 siRNA knockdown studies

The SOX6 gene was knocked down before differentiation and before each cycle of the adipocyte induction process in insulin media. ON-TARGETplus Human SOX6 siRNA SMARTpool (Dharmacon, L-015101-01-0050), ON-TARGETplus Mouse Sox6 siRNA SMARTpool (Dharmacon, L0442910-01-0050) or ON-TARGETplus Non-targeting Pool siRNA (Dharmacon, D-001810-10-50) at a final concentration of 100nM. Transfections were conducted using Lipofectamine RNAiMAX (Invitrogen, 13778150).

SOX6 over-expression study

For the over-expression of Sox6, 3T3L1 cells were transfected using Lipofectamine LTX (Invitrogen) with 2.5 µg GFP-tagged plasmid containing the mouse Sox6 gene (MG227129; Origene Technologies) in 6cm dishes. This transient transfection was performed before differentiation and every 2 days during differentiation.

Luciferase reporter assay

For the WNT activity reporter assay, HEK293 cells were cultured in growth medium (DMEM high glucose with 2 mM L-glutamine, 10% FBS, antibiotic/antimycotic mixture). Cells seeded in 6-well plates were co-transfected with 1000ng of SuperTOP-FLASH (Addgene, plasmid #12456), 100ng of pTK–Renilla luciferase (Promega, E2241) and 1500ng GFP-tagged plasmid containing the human SOX6 gene (Origene Technologies, RG211525). For the PPARγ reporter assay, 3T3L1 cells were co-transfected with 1000ng of PPRE-X3-TK-luc (Addgene, plasmid #1015) and 100ng of pTK-Renilla luciferase. All assays were conducted following the dual-luciferase assay protocols (Promega, E1910). TOP-FLASH activity was normalized against Renilla luciferase readout. For the MEST reporter assay, 3T3L1 cells were co-transfected with 1000ng of custom-made GLuc_ON MEST Promoter Reporter using pEZX-PG04 vector (GeneCopoeia, MPRM26666-PG04). Assays were

performed in agreement with the Secrete-Pair Gaussia Luciferase Dual Assay Kit (GeneCopoeia, SPDA-D010). Secreated alkaline phosphatase luciferase activity was used to normalize Gaussia Luciferase- (GLuc-) MEST promoter activity.

Pyrosequencing

Genomic DNA was prepared and converted with bisulfite using the EpiTect Bisulfite Kit (Qiagen) according to manufacturer's recommendations. Pyrosequencing was performed using a PyroMark Q24 machine (Qiagen) in 10-15µL of PCR product in a standard reaction volume. The sequences of PCR and sequencing primers are provided in supplementary material Table S3.

Electrophoretic mobility shift assay (EMSA)

EMSA was performed using the Odyssey Infrared EMSA kit (LICOR, Part No: 829-07910). Varying concentration of human recombinant SOX6 protein (Origene, TP312046) were incubated for 20 minutes at room temperature with a synthetic SOX6 oligonucleotide 5' end-labeled with IRDye 700 with or without 5-methyl-dC modification at the CpG motif (double stranded, 5'- TTA TTC TCT TTA TCC AAT GCC GGA GGC TAT- 3') and a binding mix following the manufacturer's protocol. Separation of the reaction was performed on a 6% non-denaturing polyacrylamide gel in 0.5X cold TBE buffer (pH 8).

Gene-expression Microarray

Differential gene expression levels in liver tissue comparing SOX6 and control ASOs were determined by employing the HumanHT-12 v4 Expression BeadChip technology (Illumina, BD-103-0204). The Illumina iScan system was used for scanning the arrays followed by data extraction using the Illumina Genome Bead Studio TM Software. After background subtraction, p-values <0.05 and NBEADS>3 using the R program were determined. Afterwards, the data were further analyzed with Arraystudio (Omicsoft). Probes that passed signal detected p-value <0.05 in all the samples were retained. Log 2 transformation (intensity values <1 censored to 0) was performed followed by Quantile normalization. One-way ANOVA (~t–test) was performed to determine differential gene-

expression. All gene expression microarray data were deposited into the GEO repository (GEO #GSE70300).

Statistics

Data are generally presented as means ± S.E.M. from different biological experiments. Experiments involving comparisons between groups and time courses, for example the adipogenesis differentiation assays involving different stages (cycles) were analyzed via repeated measures analysis of variance (ANOVA). All normal comparisons between groups were assessed using a Student's t-test, with p-values <0.05 generally being considered as significant.

Acknowledgements

We are grateful for the expert technical assistance of Jun Hao Tan, Maggie Lim, Ge Xiaojia and Sathiakumar Durgalakshmi.

Competing interests

The authors declare no competing or financial interests.

Author contributions

S.C.L.: performed the experiments, conception and design, data collection and analysis and interpretation;

J.P, P.G.T, J.Y, R.J., C.M., S.P.: performed the experiments, data collection and analysis; S.D.: data analysis; A.S., K.L.N., P.W.I., M.K.L., Y.S.L., Y.S.C., P.D.G.: clinical and biological specimen collection, manuscript editing; W.S.: conception and design, data analysis, manuscript writing.

Funding

This research is supported by the Singapore National Research Foundation under its Translational and Clinical Research (TCR) Flagship Programme and administered by the Singapore Ministry of Health's National Medical Research Council (NMRC), Singapore- NMRC/TCR/004-NUS/2008; NMRC/TCR/012-NUHS/2014. SICS Investigators are supported through Agency for Science Technology and Research (A*STAR) funding. No potential conflicts of interest relevant to this article were reported.

References

Batista-Brito, R., Rossignol, E., Hjerling-Leffler, J., Denaxa, M., Wegner, M., Lefebvre, V., Pachnis, V., Fishell, G. (2009). The cell-intrinsic requirement of Sox6 for cortical interneuron development. *Neuron* **63,** 466-481

Bhurosy, T., Jeewon, R. (2014). Overweight and obesity epidemic in developing countries: a problem with diet, physical activity, or socioeconomic status? *ScientificWorldJournal*. doi: 10.1155/2014/964236

Carless, M. A., Kulkarni, H., Kos, M. Z., Charlesworth, J., Peralta, J. M., Göring, H. H., Curran, J. E., Almasy, L., Dyer, T. D., Comuzzie, A. G., et al. (2013). Genetic effects on DNA methylation and its potential relevance for obesity in Mexican Americans. *PLoS One.* doi: 10.1371/journal.pone.0073950

Cho, H. M., Lee, H. A., Kim, H. Y., Lee, D. Y., Kim, I. K. (2013). Recruitment of specificity protein 1 by CpG hypomethylation upregulates Na^+-K^+-$2Cl^-$ cotransporter 1 in hypertensive rats. *Hypertens.* **7,** 1406-13

Considine, R.V, Sinha, M.K., Heiman, M.L., Kriauciunas, A., Stephens, T.W., Nyce, M.R., Ohannesian, J.P., Marco, C.C., McKee, L.J., Bauer, T.L., et al. (1996). Serum immunoreactive-leptin concentrations in normal-weight and obese humans. *N Engl J Med* **334**, 292–295

Desai, M., Gayle, D., Babu, J., Ross, M. G. (2005). Programmed obesity in intrauterine growth-restricted newborns: modulation by newborn nutrition. *Am J Physiol Regul Integr Comp Physiol* **288,** R91-96.

de Rooij, S. R., Painter, R. C., Holleman, F., Bossuyt, P. M,, Roseboom, T, J. (2007). The metabolic syndrome in adults prenatally exposed to the Dutch famine. *Am J Clin Nutr* **86,** 1219-1224

Dumitriu, B., Patrick, M. R., Petschek, J. P., Cherukuri, S., Klingmuller, U., Fox, P. L., Lefebvre, V. (2006). Sox6 cell-autonomously stimulates erythroid cell survival, proliferation, and terminal maturation and is thereby an important enhancer of definitive erythropoiesis during mouse development. *Blood* **108,** 1198-1207

El Hajj, N., Pliushch, G., Schneider, E., Dittrich, M., Müller, T., Korenkov, M., Aretz, M., Zechner, U., Lehnen, H., Haaf, T. (2013). Metabolic programming of MEST DNA methylation by intrauterine exposure to gestational diabetes mellitus. *Diabetes* **62,** 1320-1328

Flynn, E. J., Trent, C. M., Rawls, J. F. (2009). Ontogeny and nutritional control of adipogenesis in zebrafish (Danio rerio). *J Lipid Res.* **8,** 1641-52

Fong, C. Y., Subramanian, A., Biswas, A., Gauthaman, K., Srikanth, P., Hande, M. P., Bongso, A. (2010). Derivation efficiency, cell proliferation, freeze-thaw survival, stem-cell properties and differentiation of human Wharton's jelly stem cells. *Reprod Biomed* **21,** 391-401

Godfrey, K. M., Barker, D. J. (2001). Fetal programming and adult health. *Public Health Nutr* **4,** 611-624

Godfrey, K. M., Sheppard, A., Gluckman, P. D., Lillycrop, K. A., Burdge, G. C., McLean, C., Rodford J., Slater-Jefferies, J. L., Garratt, E., Crozier, S. R., et al. (2011). Epigenetic gene promoter methylation at birth is associated with child's later adiposity *Diabetes.* **60,** 1528-34

Hagiwara, N., Yeh, M., Liu, A. (2007). Sox6 is required for normal fiber type differentiation of fetal skeletal muscle in mice. *Dev Dyn* **236,** 2062-2076

Hanson, M. A., Gluckman, P. D. (2014) Early developmental conditioning of later health and disease: physiology or pathophysiology? *Physiol Rev.* **94,** 1027-76

Iguchi, H., Ikeda, Y., Okamura, M., Tanaka, T., Urashima, Y., Ohguchi, H., Takayasu, S., Kojima N., Iwasaki, S., Ohashi, R., Jiang, S., et al. (2005). SOX6 attenuates glucose-stimulated insulin secretion by repressing PDX1 transcriptional activity and is down-regulated in hyperinsulinemic obese mice. *J Biol Chem.* **280,** 37669-37680

Jackson, H. E., Ono, Y., Wang, X., Elworthy, S., Cunliffe, V. T., Ingham, P. W. (2015). The role of Sox6 in zebrafish muscle fiber type specification. *Skelet Muscle.* **5,** doi: 10.1186/s13395-014-0026-2

Joseph, R., Poschmann, J., Sukarieh, R., Too, P. G., Julien, S. G., Xu, F., The, A. L., Holbrook, J. D., Ng, K. L., Chong, Y. S., et al. (2015). ACSL1 is associated with fetal programming of insulin sensitivity and cellular lipid content. *Mol Endocrinol* **29,** 909-20

Jung, H., Lee, S. K., Jho, E. H. (2011). Mest/Peg1 inhibits WNT signalling through regulation of LRP6 glycosylation. *Biochem J.* **436,** 263-9

Kamei, Y., Suganami, T., Kohda, T., Ishino, F., Yasuda, K., Miura, S., Ezaki, O., Ogawa, Y. (2007). Peg1/Mest in obese adipose tissue is expressed from the paternal allele in an isoform-specific manner. *FEBS Lett.* **581,** 91-6

Khandelwal, P., Jain, V., Gupta, A. K., Kalaivani, M., Paul, V. K. (2014). Association of early postnatal growth trajectory with body composition in term low birth weight infants. *J Dev Orig Health Dis.* **5,** 189-96

Kennell, J. A., MacDougald, O. A. (2005). WNT signaling inhibits adipogenesis through beta-catenin-dependent and -independent mechanisms. *J Biol Chem.* **280,** 24004-10

Kensara, O. A., Wooton, S. A., Phillips, D. .I, Patel, M., Hoffman, D. J., Jackson, A. A., Elia, M. Hertfordshire Study Group. (2006). Substrate-energy metabolism and metabolic risk factors for cardiovascular disease in relation to fetal growth and adult body composition. *Am J Physiol Endocrinol Metab.* **291,** E365-71

Lackland, D.T., Bendall, H.E., Osmond, C., Egan, B.M., Barker, DJ. (2000). Low birth weights contribute to high rates of early-onset chronic renal failure in the Southeastern United States. *Arch Intern Med.* **160**, 1472-6.

Lefebvre, V., Behringer, R. R., de Crombrugghe, B. (2001). L-Sox5, Sox6 and Sox9 control essential steps of the chondrocyte differentiation pathway. *Osteoarthritis Cartilage* **9,** S69-75

Lefterova, M. I., Haakonsson, A. K., Lazar, M. A., Mandrup, S. (2014). PPARγ and the global map of adipogenesis and beyond. *Trends Endocrinol Metab.* **25,** 293-302

Li, W., Zhu, C., Li, Y., Wu, Q., Gao, R. (2014). Mest attenuates CCl4-induced liver fibrosis in rats by inhibiting the WNT/β-catenin signaling pathway. *Gut Liver*. **8,** 282-91

Maury, E., Brichard, S.M. (2010). Adipokine dysregulation, adipose tissue inflammation and metabolic syndrome. *Mol Cell Endocrinol* **314**, 1–16

Ng, M., Fleming, T., Robinson, M., Thomson, B., Graetz, N., Margono, C., Mullany, E.C., Biryukov, S., Abbafati, C., Abera, S.F., et al. (2014). Global, regional, and national prevalence of overweight and obesity in children and adults during 1980-2013: a systematic analysis for the Global Burden of Disease Study 2013. *Lancet.* **384**, 766-81. doi: 10.1016/S0140-6736(14)60460-8.

Rosen, E. D., Hsu, C. H., Wang, X., Sakai, S., Freeman, M. W., Gonzalez, F. J., Spiegelman, B. M. (2002). C/EBPalpha induces adipogenesis through PPARgamma: a unified pathway. *Genes Dev* **16:** 22-26

Ross, S. E., Hemati, N., Longo, K. A., Bennett, C. N., Lucas, P. C., Erickson, R. L., MacDougald, O. A. (2000). Inhibition of adipogenesis by WNT signaling. *Science* **289,** 950-953

Smits, P., Li, P., Mandel, J., Zhang, Z., Deng, J. M., Behringer, R. R., de Crombrugghe, B., Lefebvre V. (2001). The transcription factors L-Sox5 and Sox6 are essential for cartilage formation. *Dev Cell* **1,** 277-290

Soubry, A., Murphy, S. K., Wang, F., Huang, Z., Vidal, A. C., Fuemmeler, B. F., Kurtzberg, J., Murtha, A., Jirtle, R. L., Schildkraut, J. M., et al. (2015). Newborns of obese parents have altered DNA methylation patterns at imprinted genes. *Int J Obes (Lond)* **39,** 650-657

Stolt, C. C., Schlierf, A., Lommes, P., Hillgärtner, S., Werner, T., Kosian, T., Sock, E., Kessaris, N., Richardson, W. D., Lefebvre, V., et al. (2006). SoxD proteins influence multiple stages of oligodendrocyte development and modulate SoxE protein function. *Dev Cell* **11,** 697-709

Sukarieh, R., Joseph, R., Leow, S. C., Li ,Y., Löffler, M., Aris, I. M., Tan, J. H., The, A. L., Chen, L., Holbrook, J. D., Ng, K. L., et al. (2014). Molecular pathways reflecting poor intrauterine growth are found in Wharton's jelly derived Mesenchymal Stem Cells. *Hum Reprod* **29,** 2287-301

Takahashi, M., Kamei, Y., Ezaki, O. (2005). Mest/Peg1 imprinted gene enlarges adipocytes and is a marker of adipocyte size. *Am J Physiol Endocrinol Metab*. **288,** E117-24

Tian, J.Y., Cheng, Q., Song, X.M., Li, G., Jiang, G.X., Gu, Y.Y., Luo, M. (2006). Birth weight and risk of type 2 diabetes, abdominal obesity and hypertension among Chinese adults. *Eur J Endocrinol.* **155**, 601-7.

van Dijk, S. J., Molloy P. L., Varinli, H., Morrison, J. L., Muhlhausler, B. S., Members of EpiSCOPE. (2015). Epigenetics and human obesity. *Int J Obes (Lond).* **39,** 85-97

Varvarigou, A. A. (2010). Intrauterine growth restriction as a potential risk factor for disease onset in adulthood. *J Pediatr Endocrinol Metab* **23,** 215-224

Vidal, A. C. Benjamin Neelon, S. E., Liu, Y., Tuli, A. M., Fuemmeler, B. F., Hoyo, C., Murtha, A. P., Huang, Z., Schildkraut, J., Overcash, F., et al. (2014). Maternal stress, preterm birth, and DNA methylation at imprint regulatory sequences in humans. *Genet Epigenet.* **14,** 37-44

Voigt, A., Ribot, J., Sabater, A. G., Palou, A., Bonet, M. L., Klaus, S. (2015). Identification of Mest/Peg1 gene expression as a predictive biomarker of adipose tissue expansion sensitive to dietary anti-obesity interventions. *Genes Nutr*. **10,** 477

Figures

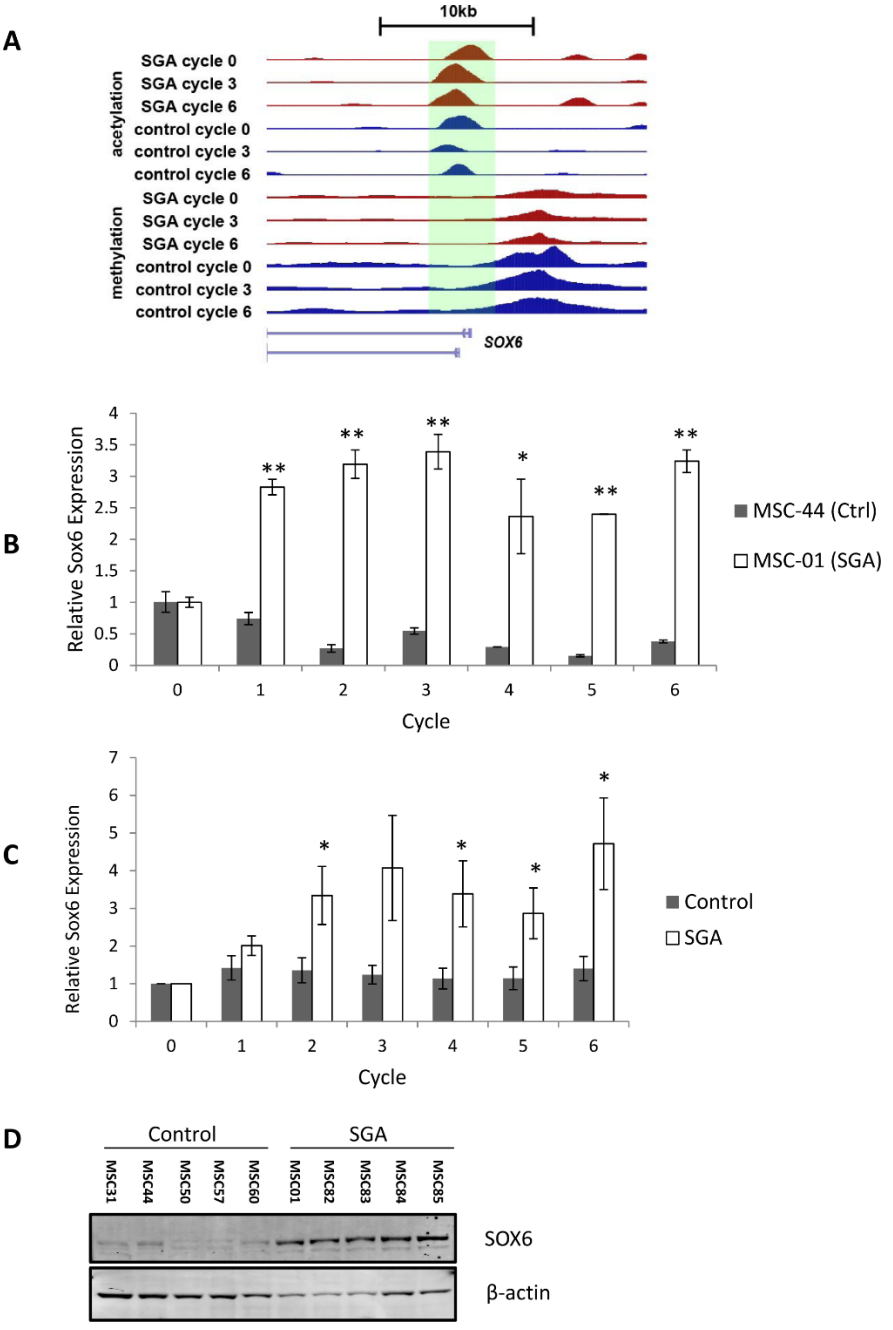

Figure 1. Higher expression of SOX6 in mature adipocytes from SGA-derived MSCs.

(A) UCSC genome browser view of SGA (MSC-01; red), control (MSC-44; blue) H3K27ac and H3K27me3 ChIP-seq signals around the SOX6 gene locus. Shown are wiggle tracks of normalized read counts. The arrow displays the gene start, length and direction. (B) mRNA expression levels of SOX6 in adipocytes from MSC-01 (SGA) compared to MSC-44 (control) determined by RT-qPCR. Results are representative of 3 independent experiments. Data are shown as mean fold change ± SEM for SOX6 expression relative to that of MSC-44 cycle 0 sample. A two-way ANOVA analysis was performed to show the significant difference in effect of differentiation cycles ($p < 0.0001$) and MSC lines ($p < 0.0001$) for gene expression between biological repeats followed by Student's t test (*=$p < 0.05$, **=$p < 0.01$). (C) SOX6 mRNA expression in an extended group of SGA (n=8) and control (n=5) MSC lines. Data are shown as mean fold change ± SEM for SOX6 expression relative to control lines at cycle 0. A two-way ANOVA analysis was performed to show the significant difference in effect of differentiation cycles ($p=0.0493$) and sample groups ($p<0.0001$) for gene expression between MSC lines followed by a Student's t test (*=$p < 0.05$, **=$p < 0.01$). (D) SOX6 protein expression is significantly higher in mature adipocytes from SGA derived MSCs.

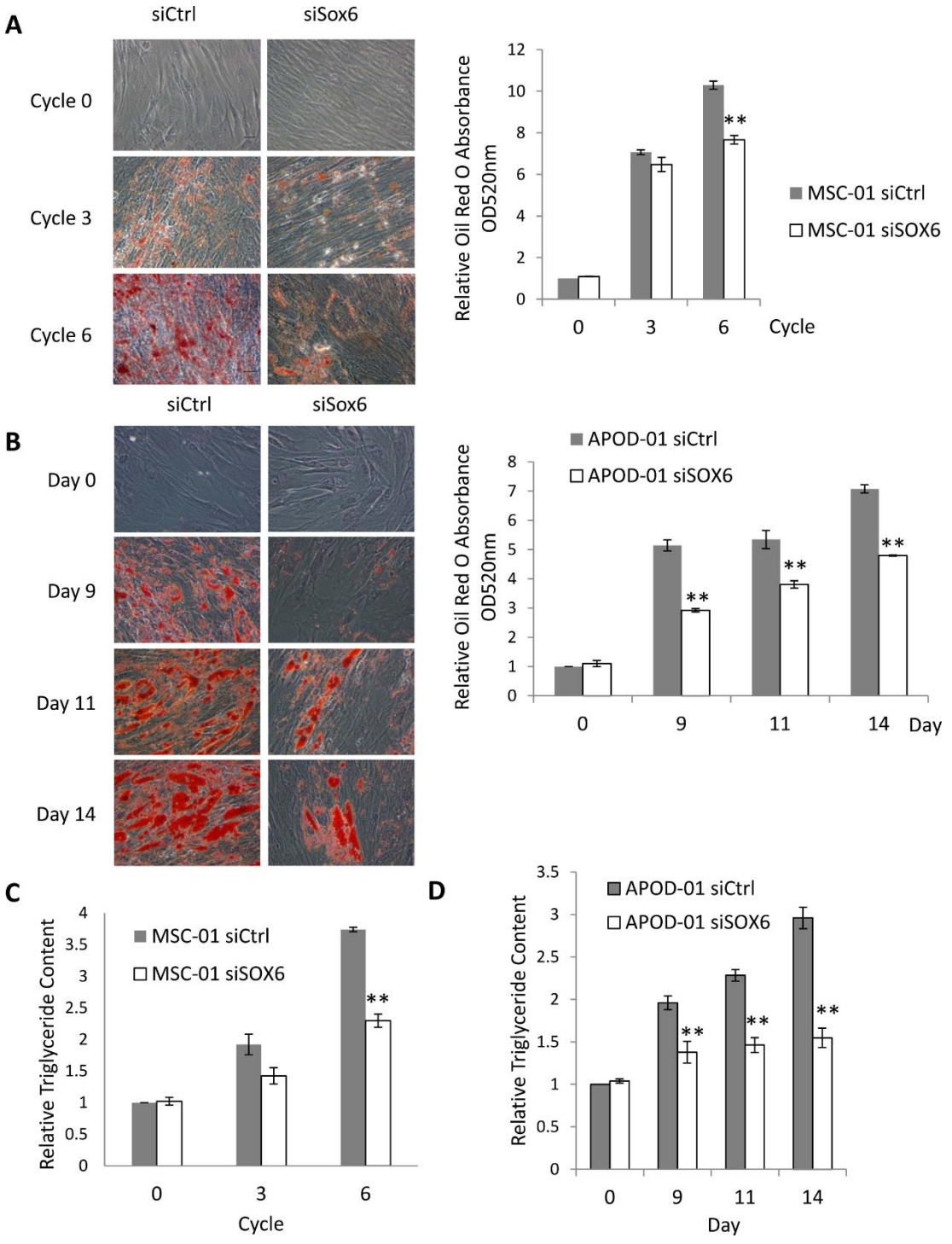

Figure 2. SOX6 down-regulation impairs adipogenesis.

(A, B) MSC-01 and APOD-01 cells at different stages of differentiation. Images are representatives of 3 independent experiments. Right panels depict the quantification of Oil Red O absorption by spectrophotometry. Data represent the mean relative absorbance ± SEM compared with siCtrl cycle/day 0 (n=3, **=p<0.01). (C, D) The amount of total triglycerides in siCtrl-treated or siSOX6-treated MSC-01 and APOD-01 cells were measured in triplicates and normalized against their total protein content in three separate experiments. Data are shown as mean ± SEM, relative to siCtrl cycle/day 0. A two-way ANOVA was performed to show significant difference in time points ($p < 0.0001$) and between siRNA treatment ($p < 0.0001$ for MSC-01 and APOD-01) over triglyceride content followed by a Student t-test (*=p<0.05, **p<0.01).

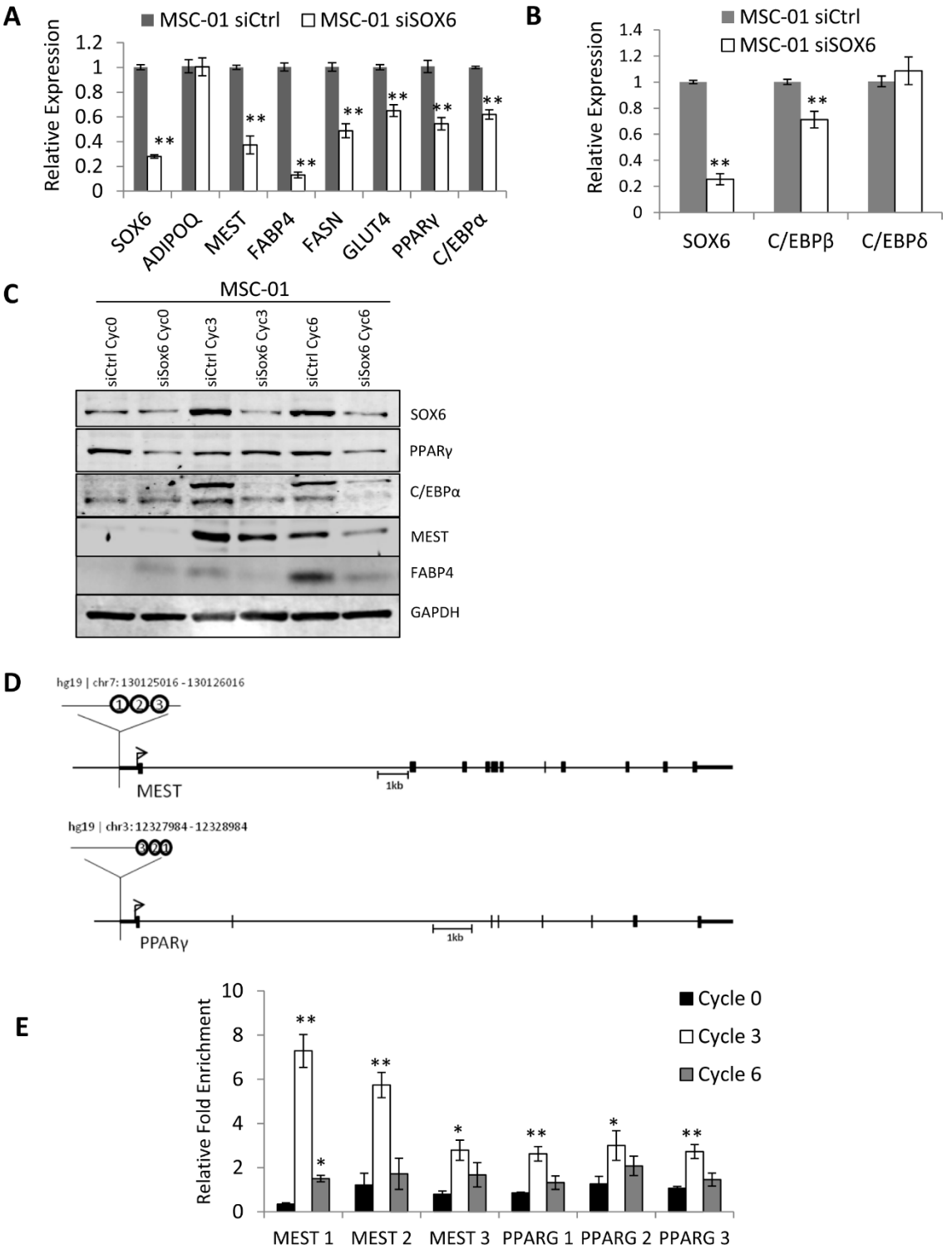

Figure 3. SOX6 regulates the expression of key adipogenic genes.

(A, B) mRNA expression levels of adipocyte markers, ADIPOQ, MEST, FABP4, FASN, GLUT4 and adipogenic regulators, PPARγ, C/EBPα, C/EBPβ and C/EBPδ were determined by RT-qPCR in MSC-01 siSOX6 treated cells in comparison with the control group (siCtrl) at cycle 6 of adipocyte differentiation. Data are shown as mean ± SEM of 3 independent experiments. p-values were calculated by Student t-test's analysis (**=p< 0.01). (C) Protein expression of SOX6 and adipogenic markers in siCtrl- and siSOX6-treated MSC-01 cells. (D, E) SOX6 enrichment at the MEST and PPARγ promoters was measured by ChIP-qPCR at cycles 0, 3 and 6 of the adipocyte differentiation in MSC-01 cells. Data are shown as mean fold enrichment ± SEM of three independent experiments and were normalized against IgG enrichment and against a negative control site (SOX4). p-values were calculated by Student t-test's analysis (*=p<0.05, **=p< 0.01).

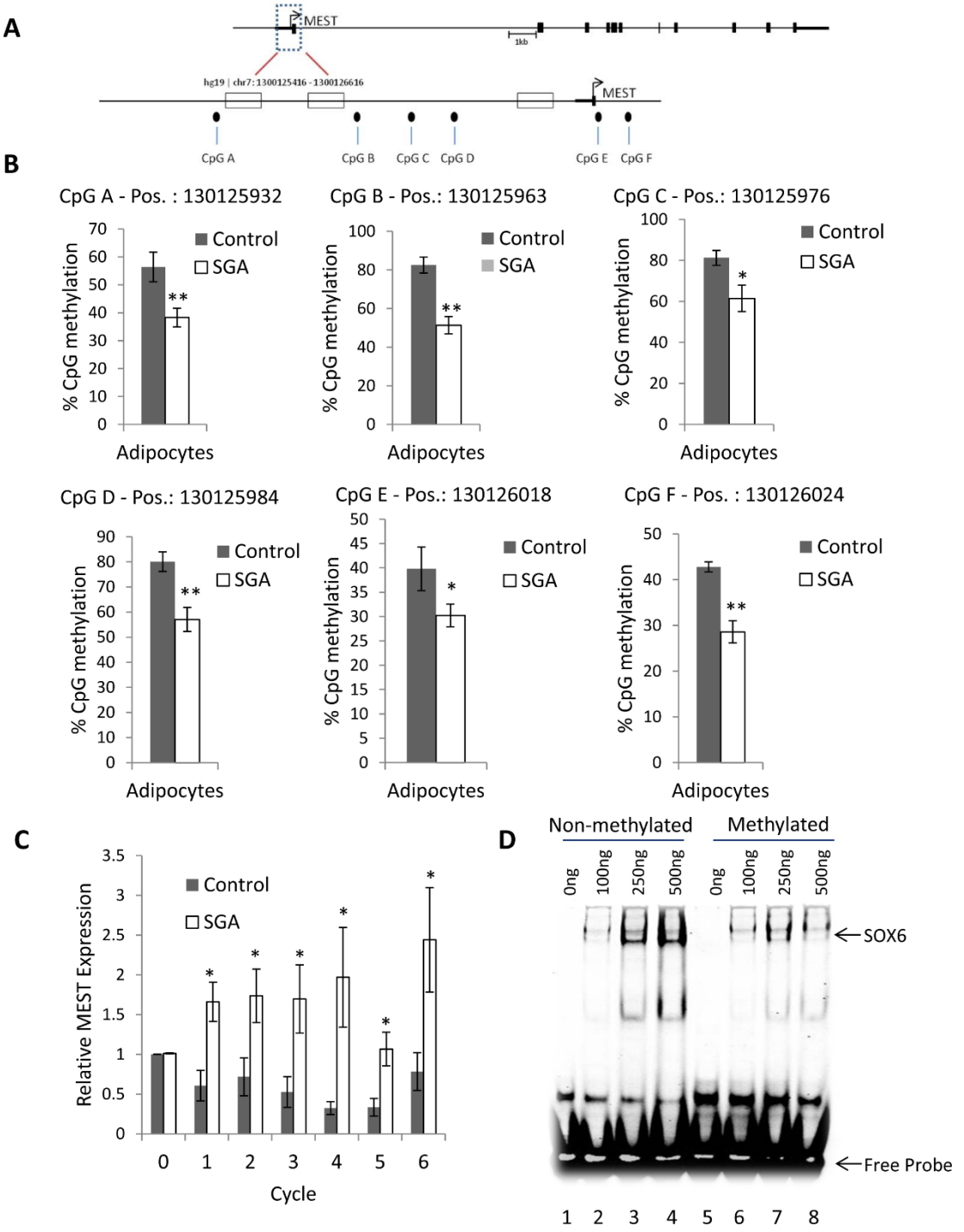

Figure 4. CpGs next to SOX6 binding sites within the MEST upstream regulatory region are hypo-methylated in SGA derived differentiated adipocytes and CpG methylation interferes with SOX6 binding.

(A) Map of the MEST region next to the transcriptional start site covering three SOX6 binding sites (open boxes) surrounded by 6 CpGs (closed circles), which were selected for pyrosequencing. (B) Percentage of CpG methylation for each of the 6 individual CpGs described in A. Genomic locations of the CpGs A-F are given above the subpanel figures. A group of control adipocyte lines (n=5) were compared with those from a group of SGA lines (n=7). Data are presented as mean ± SEM and for the statistical analysis, p-values were calculated by a Student t-test (**=p< 0.01; *= p< 0.05). (C) MEST mRNA expression in the group of SGA (n=7) and control (n=5) MSC lines as measured by qPCR. Data are shown as mean fold change ± SEM for MEST expression relative to control lines at cycle 0. A two-way ANOVA analysis was performed to show the significant difference in sample groups ($p<0.0001$) for gene expression between the groups of MSC lines followed by a Student's t test (*=$p<0.05$). (D) EMSA with human recombinant SOX6 protein at increasing concentrations and a MEST-promoter-based oligonucleotide comprising site "CpG B" as shown in A, either methylated or non-methylated and harboring a putative SOX6 binding site.

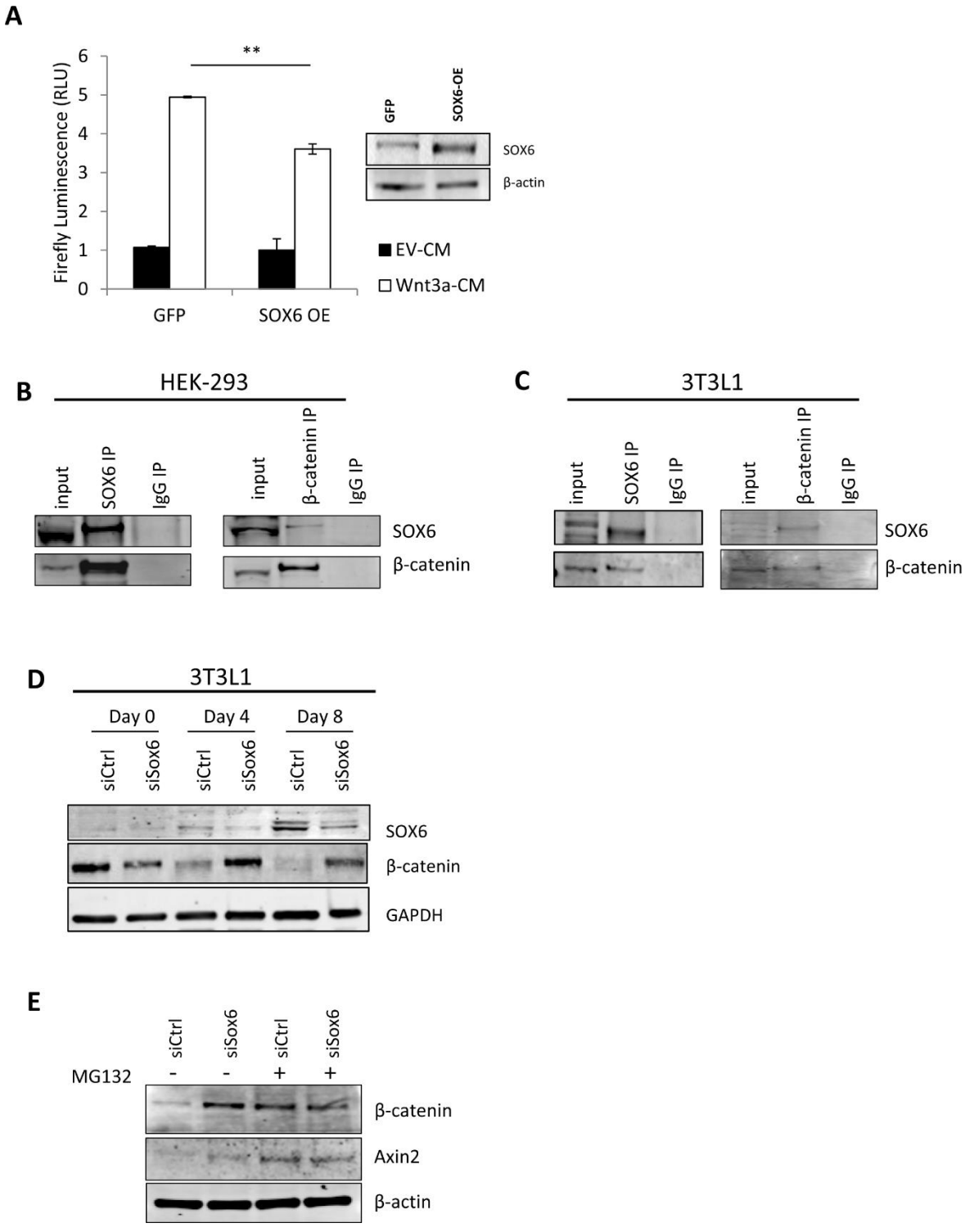

Figure 5. Regulation of WNT pathway by SOX6.

(A) SOX6 inhibited TOP-FLASH activity induced by WNT3a-conditioned medium (WNT3a-CM). HEK-293 cells co-transfected with both a GFP or SOX6 expression plasmid (labelled as "SOX6 OE") and TOP-FLASH reporter were incubated with the empty vector conditioned medium (EV-CM) or WNT3a-CM for 16h, followed by luciferase assays (left panel). Data are shown as mean RLU ± SEM compared against cells in EV-CM. p-values were calculated by two-way ANOVA analysis (**=p< 0.01). The right panel exerts a western blot experiment showing the protein expression of SOX6 after transfection. (B, C) Immunoprecipitations from HEK-293 with ectopic SOX6 expression (B) or 3T3L1 cells (C) with SOX6 antibody (left panels) or β-catenin antibody (right panels) show association of β-catenin with SOX6. Controls were samples immunoprecipitated with preimmune mouse or rabbit IgG (IgG). IP: immunoprecipitating antibody. (D) siRNA mediated downregulation of SOX6 leads to an increase in β-catenin protein expression in 3T3L1 differentiated adipocytes. (E) The reduction of β-catenin protein by SOX6 in 3T3L1 adipocytes is based on proteasomal degradation. Alteration of β-catenin and Axin2 levels by Sox6 siRNA in the presence of 2μM of the proteasome inhibitor MG132 (lanes 3 and 4 from the left) and its absence (lanes 1 and 2).

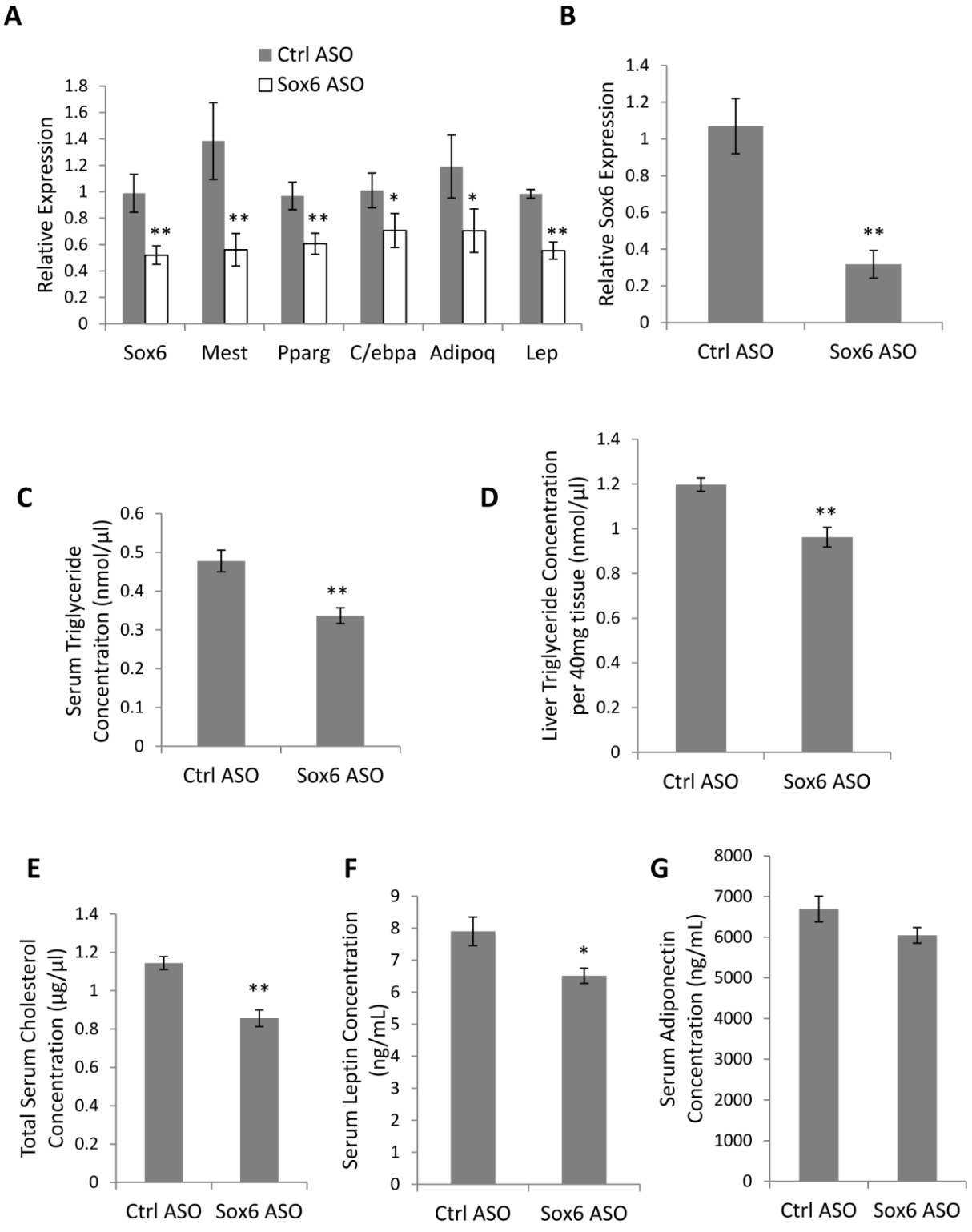

Figure 6. Decreased lipid levels in mice following SOX6 ASO treatment.

(A) Mice (n = 9 animals per group) on a chow diet were treated with control or Sox6 ASO (50mg/kg/week) by i.p. injection for a week. mRNA expression of Sox6 and selected adipogenic genes in EWAT after ASO treatment. (B) mRNA expression of Sox6 in the liver of ASO treated mice. (C-E) Serum and liver triglyceride, as well as serum cholesterol levels were found to be reduced in mice treated with Sox6 ASOs. (F, G) Serum levels of leptin and adiponectin levels in control and Sox6 ASO-treated mice p-values were calculated by Student t-test's analysis (*=$p<0.05$, **=$p< 0.01$).

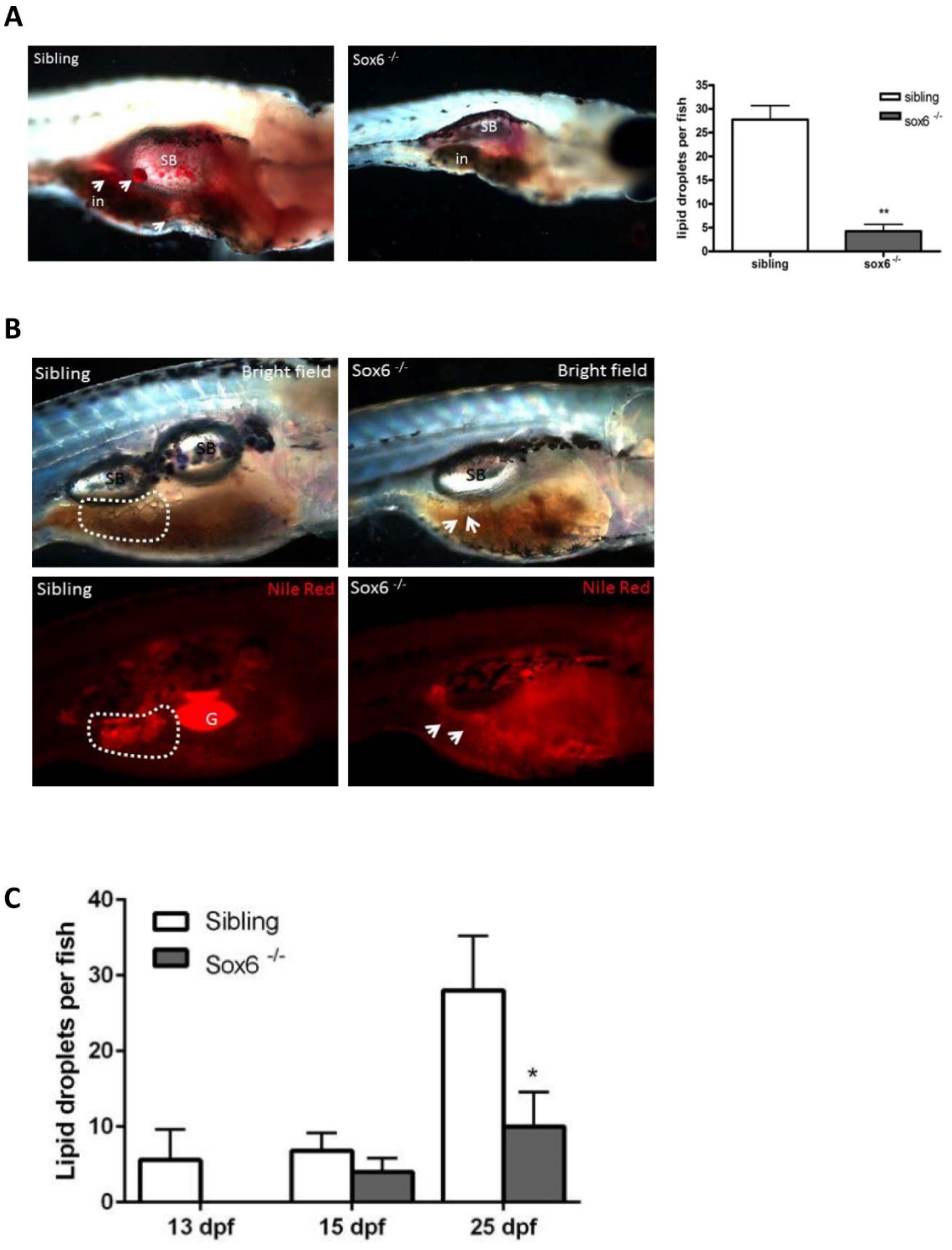

Figure 7. Sox6 mutant zebrafish larvae exert decreased adipogenesis.

(A) Oil Red O staining reveals localization of adipocyte neutral lipid droplets in larvae at 23 days post fertilization (dpf). The arrows indicate the localization of adipocytes. The number and size of neutral lipid droplets are decreased in Sox6 mutants (middle panel). Swim bladder (sb) and intestine (in) are indicated. Anterior is to the right and dorsal at the top in all images. Student's two-tailed, unpaired t-test $p < 0.05$, error bars represent standard deviation, sibling n = 4, mutant n = 4, ** $p < 0.01$.

(B) Nile Red staining revealing that adipocyte lipid droplets are decreased in number and size within the viscera of Sox6 mutant larvae at 25 dpf. Bright-field (upper panel) and corresponding fluorescence images (lower panel) are shown. Swim bladder (sb) and gall bladder (G) are indicated. The arrows indicate the localization of adipocytes (dotted line). Anterior is to the right and dorsal at the top in all images. (C) Live larvae at 13, 15, and 25 dpf were stained with Nile Red. The number of lipid droplets is decreased in Sox6 mutant larvae at all developmental stages. Student's two-tailed, unpaired t-test $P < 0.05$, error bars represent standard deviation, sibling n = 4, mutant n = 4, * $p < 0.05$.

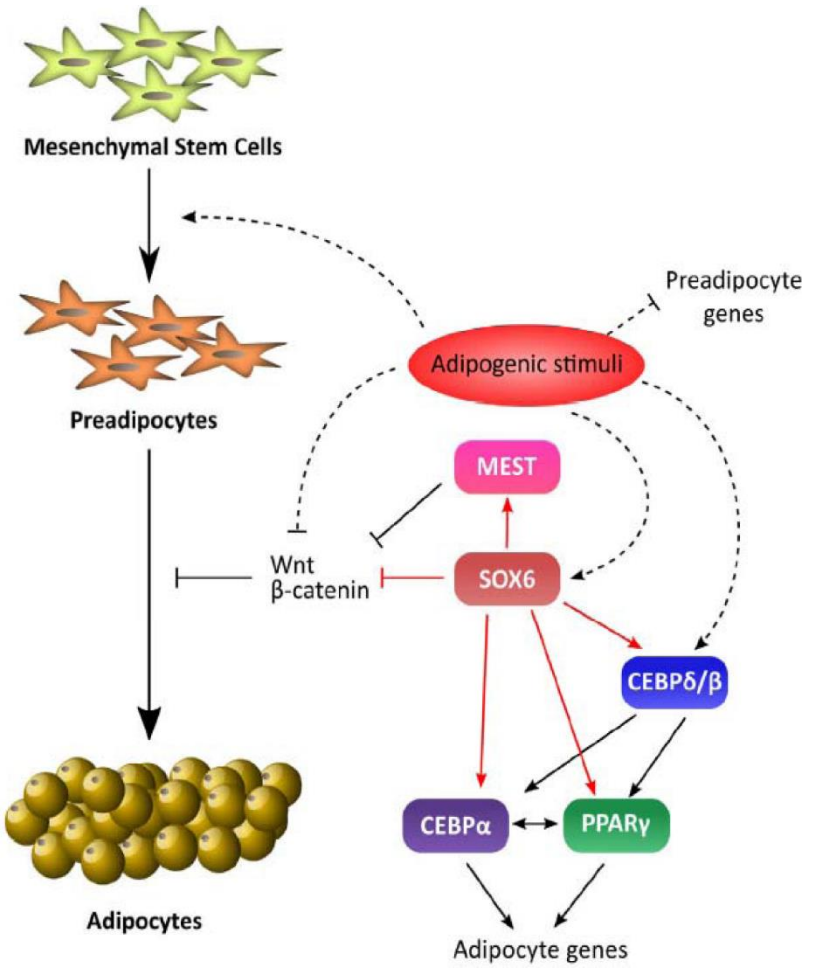

Figure 8. Model of SOX6 regulating adipogenesis.

SOX6 activates adipogenesis by directly promoting the expression of C/EBPs and PPARγ. In addition, SOX6 binds to the MEST promoter thereby activating its expression, which in response inhibits WNT signaling. SOX6 also directly binds to β-catenin leading to its degradation, which further blocks WNT signaling promoting adipocyte differentiation.